Understanding the Impact of Cutting in Quantum Circuits Reliability to Transient Faults

2022 IEEE 28th International Symposium on On-Line Testing and Robust System Design (IOLTS) | 978-1-6654-7355-2/22/$31.00 ©2022 IEEE | DOI: 10.1109/IOLTS56730.2022.9897308

Understanding the Impact of Cutting in Quantum Circuits Reliability to Transient Faults

Nadir Casciola*, Edoardo Giusto*, Emanuele Dri*, Daniel Oliveira†, Paolo Rech‡, Bartolomeo Montrucchio*

*DAUIN, Politecnico di Torino, Torino, Italy
nadir.casciola@studenti.polito.it, edoardo.giusto@polito.it, emanuele.dri@polito.it, bartolomeo.montrucchio@polito.it
†Department of Informatics, Federal University of Paraná (UFPR), Curitiba, Brazil
dagoliveira@inf.ufpr.br
‡Department of Industrial Engineering, Università di Trento, Italy
paolo.rech@unitn.it

***Abstract*—Quantum Computing is a highly promising new computation paradigm. Unfortunately, quantum bits (qubits) are extremely fragile and their state can be gradually or suddenly modified by intrinsic noise or external perturbation. In this paper, we target the sensitivity of quantum circuits to radiation-induced transient faults. We consider quantum circuit cuts that split the circuit into smaller independent portions, and understand how faults propagate in each portion. As we show, the cuts have different vulnerabilities, and our methodology successfully identifies the circuit portion that is more likely to contribute to the overall circuit error rate. Our evaluation shows that a circuit cut can have a $4.6x$ higher probability than the other cuts, when corrupted, to modify the circuit output. Our study, identifying the most critical cuts, moves towards the possibility of implementing a selective hardening for quantum circuits.**

***Index Terms*—Quantum Computing, Fault Tolerance, Fault Injection, Reliability Evaluation, Quantum Circuit Cutting**

I. Introduction

Quantum Computing (QC) exploits quantum physics properties to increase parallelism and computation efficiency. A quantum bit (*qubit*) is not in a deterministic state (1 or 0), but in a *superposition* of states, represented on the Bloch sphere (see Figure 1). Since the state of a qubit is probabilistic, an operation on a qubit is actually applied on multiple possible values simultaneously, exacerbating parallelism.

QC has moved from being a conceptual solution for specific physics problems to a highly parallel and highly efficient computing architecture [1]–[4]. Currently, quantum computers are easily accessible in the cloud and various frameworks have been developed to allow the simulation of quantum circuits in traditional workstations [5], [6].

Unfortunately, qubits are very fragile and sensitive to both intrinsic noise and external perturbations. Extremely costly fault-tolerant solutions (that include intrinsic replication and isolation from the external environment) guarantee sufficiently stable qubits for the computation of small, yet crucial, circuits [7], [8]. Crucially, as the first quantum computers have been produced and installed in the field, it has been discovered that superconducting qubits are extremely susceptible to external radiation [9]–[12]. The impact of natural particles (neutrons but also lighter particles such as muons) undermines the stability of qubits and, on a quantum computer with only tens of qubits, natural radiation-induced events are observed every few *seconds* [13]–[15]. Ionizing radiation, which is one of the biggest challenges for modern classical computing systems, is then expected to be a major issue also for future quantum (super-) computers [10], [12].

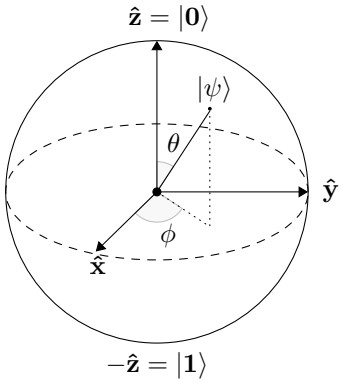

Fig. 1: Bloch sphere that visualizes the generic state of a qubit.

This paper evaluates the impact of quantum circuits cutting on transient fault propagation. Cutting is a novel technique that allows splitting the quantum circuit into various independent sub-circuits (cuts) [16], [17]. The outputs of each cut are then combined to produce the circuit result. Since the cuts have a smaller size than the original circuit, they are easier to simulate or execute, allowing to run a complex circuit even on a quantum computer with few qubits. When it comes to reliability, we believe that circuit cutting is a promising technique to be exploited for selective hardening. Our intuition is that each cut has a different vulnerability to faults. Understanding the fault propagation in the cuts, we can identify the circuit portions that, if selectively protected, are more likely to improve the circuit reliability.

The results of our experiments show that the corruption of a cut can be 4.6x more likely to modify the circuit final

978-1-6654-7355-2/22/$31.00 ©2022 IEEE

output with respect to the corruption of other cuts. The most critical cuts become the natural candidates for future selective hardening techniques aimed at increasing the circuit reliability while avoiding unnecessary overhead in terms of valuable quantum resources.

The rest of the paper is organized as follows. In Section II we provide essential background information about qubits and quantum computing, quantum noise, and radiation-induced faults. Then, in Section III, we describe circuit cutting, how it is performed and why it is relevant for the prospect of a future selective hardening technique. In Section IV, we present the experimental setup used and detail the circuits tested and their cuts. The obtained results are presented in Section V, and Section VI concludes the paper.

II. Background

This Section covers the fundamentals of quantum computing, quantum noise, and radiation-induced faults. Our aim is to give all necessary information needed to delineate the context in which the proposed work has been carried out, rather than fully cover quantum computing theory.

A. Quantum computing

The basic unit of information of a classical computer is the bit, which can take binary values, 0 or 1. Instead, the basic unit of information in quantum computing is the *qubit*. Being a two-level quantum-mechanical system, a qubit can exist in a *superposition* of states, which is a linear combination of the two basis states. A generic qubit state $|\Psi\rangle$ is defined as

$$|\Psi\rangle = \alpha\,|0\rangle + \beta\,|1\rangle \tag{1}$$

where α and β are complex numbers that represent the probability amplitude of the basis states $|0\rangle$ or $|1\rangle$. This generic state can be also identified as the vector $|\psi\rangle$ in Fig. 1, which gives a graphical representation of the state of the qubit encoded in the polar coordinates ϕ and θ.

A quantum code is executed encoding the input in the qubit state and using quantum gates to apply stimuli to the qubits. The output of the quantum computation is *probabilistic*, and not deterministic, due to the peculiarity of the quantum state of the qubit. To be physically executed on a real quantum machine, the quantum circuit has to be mapped to a certain physical architecture. This process is called *transpiling*. Current physical machines are referred to as Noisy Intermediate Scale Quantum Computers (NISQ), since they are still not meeting the fault-tolerant dependability standards.

B. Quantum noise and Radiation-Induced Faults

The physical realization of a qubit is a conundrum. The optimal stability would be achieved completely isolating the qubit from the surrounding environment, so that its state would not be affected by the intrinsic noise. However, such an isolated qubit would be much more difficult to control, perform computation on it, and read its output. A real qubit is characterized by two coherence times, $T1$ and $T2$. $T1$ is the *relaxation* time, while $T2$ is the *dephasing* time. $T1$ defines the time for which the qubit can maintain its state, so the actual data. $T2$ defines the time for which the qubit is resistant to external noise.

Quantum computing hardware providers are working closely with academics to reduce the impact of surrounding noise both on the hardware and the software point of view [18]. Physical isolation techniques and layouts are constantly being developed following the everyday findings. Quantum Error Correction (QEC) mechanisms are being developed to improve resiliency at the logical level, hoping to compensate for flawed real implementations [19].

Standard QEC techniques, however, do address only inherent machine noise. Several recent studies on superconducting qubit machines have highlighted that ionizing radiation significantly reduces quantum circuit reliability, clearly showing the criticality of particles' impact with qubits, posing a threat to their application [9]–[15], [20]. A recent paper by Google AI quantified the radiation problem by performing a field measurement on a quantum processor to detect radiation-induced faults [21]. They trace transient faults both in time and space, tracking them from the impact location through their fast spread in the chip. The highly worrying aspect of Google's experiment is that radiation events corrupted qubits at an incredibly high rate. Every tens of second a radiation-induced error was detected in a tens of qubits quantum chip. This discovery is an actual call to arms to all fault tolerance and reliability experts to urgently address transient-fault issues.

To allow the evaluation of transient faults propagation in a quantum circuit the *Quantum Fault Injector (QuFI)* framework has recently been released [22]. QuFI can be used to identify the quantum circuits' sensitivity to radiation-induced faults and the probability for a fault in a qubit to propagate to the output. In *QuFI* the transient faults in a qubit are modeled as phase shifts with parameterized magnitude, tunable at will. QuFI can also inject multiple qubit faults, adapting the phase shift magnitude depending on the distance between the qubit and the particle strike location.

C. Main Idea and Contribution

In this paper, we aim at investigating the reliability of quantum circuit cutting. The ultimate scope of the evaluation is to understand the possibility of exploiting circuit cutting to implement selective hardening in quantum circuits. Circuit cutting is a new technique that allows dividing complex quantum circuits into small portions to be executed on small quantum computers. The outputs of the circuit cuts are then combined to form the original circuit output. We investigate the vulnerability to transient faults of the circuit cuts and identify the ones that are more critical for the circuit's correct execution. These are the cuts that should be protected. To the best of our knowledge, this is the first work addressing the transient fault reliability of quantum circuit cuts.

III. Circuit Cutting

Given the complexity of qubit physical implementations, the availability of qubits in NISQ devices is very low and limits

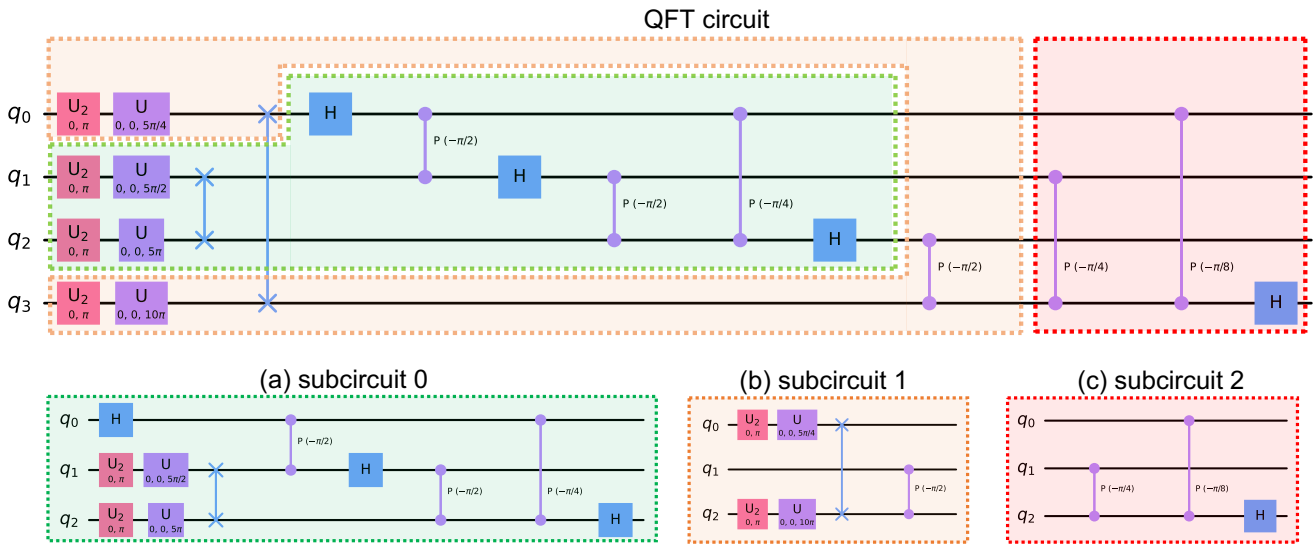

Fig. 2: Original 4-qubit QFT circuit (top) and three QFT circuit cuts of 3 qubits each (bottom). The three cuts output combination provides the original circuit output, allowing the cuts to be executed on quantum computers with fewer qubits.

the set of quantum circuits that can be effectively run. In recent years, circuit cutting emerged as a viable solution to overcome this constraint. This hybrid approach is based on cutting large quantum circuits into smaller subcircuits, allowing for their execution on smaller quantum systems. Then, a classical postprocessing step is used to reconstruct the output of the whole circuit [16]. The ability to cut quantum circuits in the first place is due to the possibility of decomposing the unitary matrix of an arbitrary quantum operation into any set of orthonormal bases [17].

The process of circuit cutting involves selecting one or more locations in the circuit where the qubit wire is cut. Then, based on these locations, a set of *subcircuits* is extracted (Figure 2). These subcircuits can now be independently executed and their outputs recombined, using a classical computation, to reconstruct the output of the full circuit. The advantage of circuit cuts lies in the fact that each subcircuit is usually smaller, in number of qubits and/or circuit depth, than the original circuit, making it possible to execute N-qubit logical circuits on physical devices with $M < N$ qubits. In Figure 2 there is an example of a 4-qubit circuit cut into three 3-qubit subcircuits.

In this paper, we present an innovative utilization of the cutting procedure. Our aim is to understand the impact of single faults on the various subcircuits, as well as the impact on the global output when one of the cuts is corrupted by a transient fault. We can then evaluate the most sensitive cuts to faults, thus identifying the best candidate for future hardening techniques, limiting the overhead necessary to guarantee that the output integrity is substantially preserved.

In this work, the selection of the circuit cut locations is done by the CutQC framework. CutQC's cut searcher automates the identification of cuts while optimizing for the least amount of classical postprocessing [16]. Once a circuit is cut, for the classical postprocessing step (i.e. the recombination of the subcircuits outputs), we use MLFT's implementation (Maximum Likelihood Fragment Tomography) of circuit cutting [23], a technique that aims to reconstruct the "most likely" probability distribution defined by a quantum circuit, given the measurement data obtained from its subcircuits.

IV. Experimental Setup

In this Section, we describe the setup used to obtain our results. First, we detail the quantum circuits tested as well as the cuts performed in each circuit. Then, we describe how to evaluate the reliability of quantum circuits and cuts.

A. Quantum Circuits and Subcircuits

We perform our analysis on the three most widely known quantum circuits, each circuit has a width of 4 qubits:

Deutsch–Jozsa (DJ) is a circuit that, given an executed function, is able to identify if the function is constant or balanced. DJ was one of the first examples of a quantum algorithm exponentially faster than a classical one [24], [25].

Bernstein–Vazirani (BV) is an extension of Deutsch–Jozsa that tries to learn a string encoded in a function [26].

Quantum Fourier Transform (QFT) is the quantum analogue of the discrete Fourier transform [27]. It applies a linear transformation to qubits and it is a part of many quantum algorithms, notably Shor's factoring algorithm and Quantum Phase Estimation (QPE).

The circuits are cut into their subcircuits using the CutQC framework, which chooses the location of the cuts automatically, optimizing for minimal classical overhead needed to reconstruct the final result [16]. The reconstruction of the final output is done using MLFT's implementation [23].

We describe the cut solutions using circuit depth and the number of operations, with circuit depth being defined as the

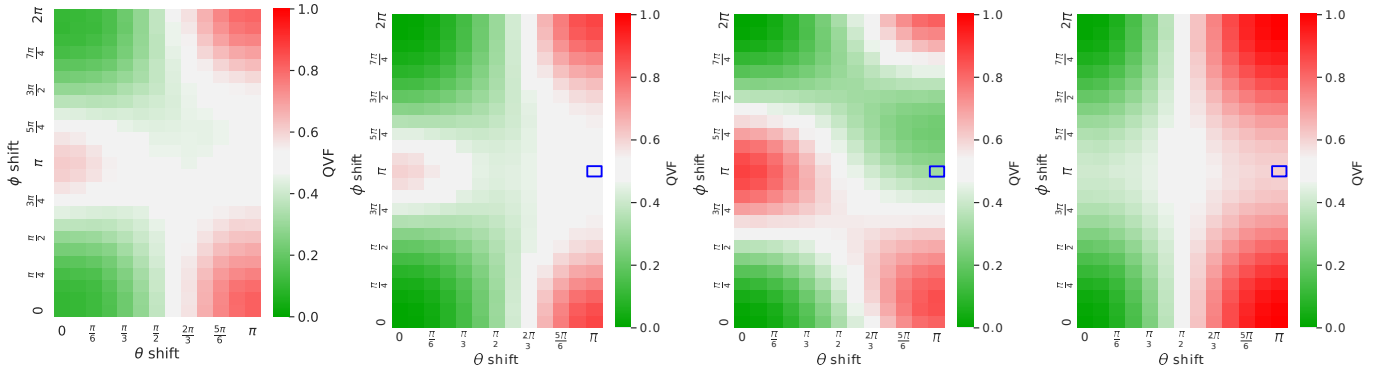

(a) Uncut QFT circuit (b) Subcircuit 0 (c) Subcircuit 1 (d) Subcircuit 2

Fig. 3: QVF heatmaps for the QFT circuit and the subcircuits produced by CutQC circuit cutting framework. The green color indicates a low QVF (the correct state can be confidently selected), the red color indicates a higher QVF (an incorrect output is more likely to be selected), and the white color indicates a dubious output (i.e., correct and incorrect states have about the same probability).

highest number of operations on a single qubit wire that can be found on the quantum circuit in consideration. As an example, in Figure 2, we show the cutting solution for the QFT circuit. From the uncut 4-qubit circuit three subcircuits of 3 qubits each are extracted (Figures 2 a, b, and c). In the subcircuits, the uncut circuit's depth of 7 is reduced to a depth of 6, 4, and 3, respectively, while the number of operations is reduced from 20 to 11, 6, and 3. Concerning our other tested circuits, BV's uncut circuit is composed of 4 qubits plus 1 ancilla qubit, with a circuit depth of 6 and a total of 14 operations. While not shown here for space constraints, the cut solution we used results in two subcircuits of 4 (*3 + 1 ancilla*) and 2 (*1 + 1 ancilla*) qubits each, with circuit depths of 5 and 3 respectively and 11 and 3 operations. Thus, this particular cut results in the first subcircuit being considerably larger than the second. The cut solution used for the DJ circuit is similar. The uncut circuit is composed of 4 qubits plus 1 ancilla qubit and is cut into two subcircuits of 4 (*3 + 1 ancilla*) and 2 (*1 + 1 ancilla*) qubits. The number of operations, 22, is divided into 17 and 5 respectively, while the circuit depth goes from 6 of the uncut circuit to 5 for both subcircuits. Hence, this also results in the first subcircuit being significantly larger than the second.

B. Reliability Evaluation

To evaluate the reliability of quantum circuits we use the Quantum Fault Injector (QuFI) [22]. A classical fault injector changes the state of the program by flipping the classical bit values from zero to one and vice versa. Instead, QuFI changes the state of a quantum bit (qubit), represented in the Bloch Sphere (as seen in Figure 1), by performing a shift in the θ and ϕ angles. The possible magnitudes range for θ and ϕ are $[0, \pi]$ and $[0, 2\pi]$ respectively. We tested all possible shift combinations discretising each angle range in steps of $\frac{\pi}{12}$, which results in 312 possible configurations (i.e., distinct phase shifts) for each fault location.

We perform an exhaustive fault injection campaign, injecting faults after each one of the circuit operations (i.e., circuit gates). This is the analogue of injecting faults after each one of the program instructions. In total, we have injected more than $23,000$ faults.

The results of the fault injection campaign are quantified using the Quantum Vulnerability Factor (QVF) [22]. The QVF metric is analogous to Architecture Vulnerability Factor (AVF) and Program Vulnerability Factor (PVF) metrics and can be used to define how confidently one can select the correct output. As for AVF and PVF, even for QVF the lower the better (values closer to 1 indicate that the fault has a higher probability to propagate to the output). In particular, a QVF lower than 0.45 indicates that the circuit correct output is the most probable one, meaning the fault has a minor impact. QVF values higher than 0.45 and lower than 0.55 indicate a dubious output, meaning the correct nor the incorrect output can be confidently selected. Finally, values higher than 0.55 indicates the incorrect output will be the most probable one, which means the fault has a harmful effect.

V. Results

In this Section, we first present a detailed analysis of the reliability of circuits and subcircuits. Then, we show how selectively hardening only one of the subcircuits would improve the circuit robustness without incurring unnecessary overhead (assuming hardening cost to be linear with the number of gates). For lack of space, we report only some of our results. The complete set of results and plots can be found in our data repository [28].

A. Fault Injection

We show our results through a series of colored heatmaps, such as the ones in Figure 3. Since we inject faults characterized by different combinations of (θ, ϕ) angles, we want to visually represent how a specific fault (θ_i, ϕ_i) occurring

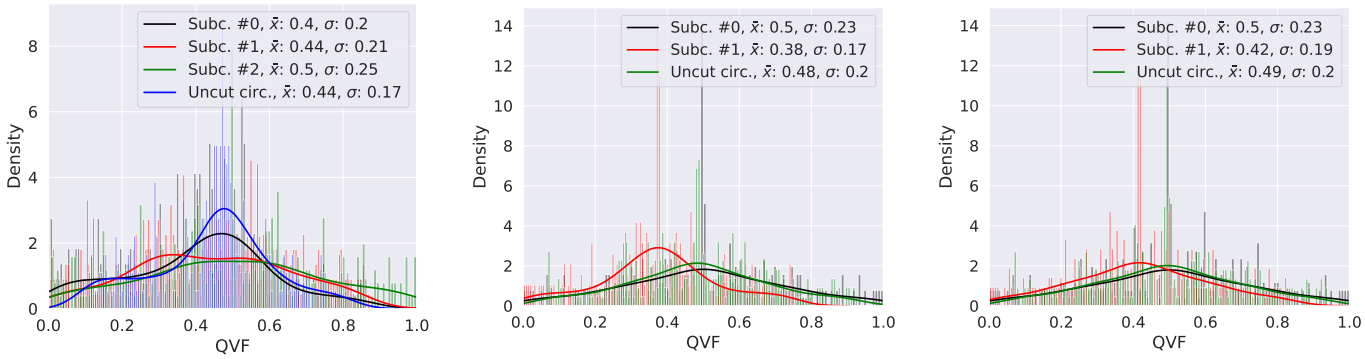

(a) QFT (b) BV (c) DJ

Fig. 4: Histograms of the QVF distribution of the three considered circuits. Lower QVF values correspond to lower probability for the fault to propagate to the final output.

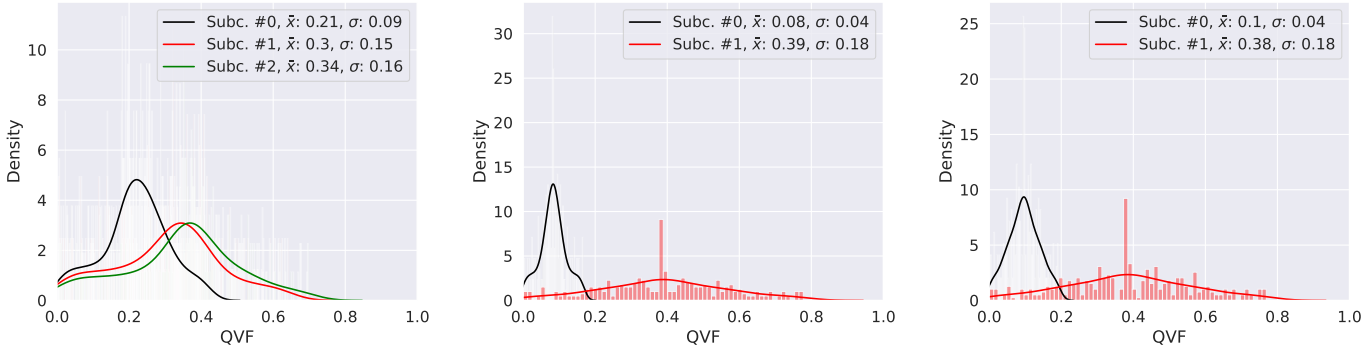

(a) QFT (b) BV (c) DJ

Fig. 5: Histograms of the QVF distribution of the three considered circuits when one of the subcircuits is selectively hardened. Even protecting just one subcircuit significantly lowers the circuit QVF (the peak is shifted to the left), indicating a lower probability for the circuit output to be corrupted.

in a given subcircuit affects the final recombined output. To do this, for each spot (θ, ϕ) we plot the average QVF value resulting from an injection of those angles in all positions of the subcircuit. In addition to the heatmaps, we also plot QVF distribution histograms to better understand a subcircuit's overall sensitivity to transient faults, such as in Figures 4 and 5. These histograms show the distribution of the QVF values (one value for each combination of (θ, ϕ)) for each subcircuit and the uncut circuit, overlapped in the same graph to better highlight the differences. The QVF mean ($\bar{x}$) and standard deviation (σ) are also shown.

The heatmaps in Figure 3 show the fault injection results for the QFT circuit and subcircuits. The faults are modeled as a θ shift (x axis) and a ϕ shift (y axis). Each spot (θ, ϕ) in the heatmaps represents the QVF mean for all possible locations for that specific fault (θ, ϕ phase shift).

Figure 3a shows the QFT sensitivity to faults for the uncut QFT circuit. We can see harmless faults (e.g., green values) only when the θ shift is lower than $\frac{\pi}{2}$. This result is justified by the fact that θ shift changes the qubit $|0\rangle$-$|1\rangle$ probability, and a shift of $\frac{\pi}{2}$ rotates the qubit vertically by half of a Bloch Sphere. Thus, a shift of $(\theta = \frac{\pi}{2})$ starts inverting the $|0\rangle$-$|1\rangle$ probability. Moreover, the combination of the ϕ and θ shift is relevant to the criticality of the fault. For instance, a shift of $(\phi = \pi, \theta = \pi)$ does not produce high QVFs (red colors) as one could expect. Thus, even if a shift in θ (i.e., a shift in the $|0\rangle$-$|1\rangle$ state probability) is indeed more critical than a shift in ϕ, the criticality from a combination of both angles cannot be easily estimated.

Each of the QFT subcircuits in Figures 3b, 3c, and 3d shows different sensitivities to injected faults. For example, a phase shift of $(\phi = \pi, \theta = \pi)$ leads to an ambiguous or incorrect output if injected in subcircuits 0 or 2 (blue squares in Figure 3b and 3d), while being tolerable for subcircuit 1 (blue square in Figure 3c). It is also worth noting that subcircuit 2 (Figure 3d) seems to be more influenced by θ shifts rather than ϕ shifts, as we can see by its heatmap having a more *vertical* pattern: faults characterized by $\theta < \frac{\pi}{2}$ tend toward being non-critical, those with $\theta \approx \frac{\pi}{2}$ produce an ambiguous output and those with $\theta > \frac{\pi}{2}$ result in an incorrect state.

Figure 4 depicts the histograms of QVF for the three circuits tested as well as the subcircuits generated, showing also the

QVF mean value ($\bar{X}$) and standard deviation (σ). Histograms provide a clear and easy way to visualize the fault injection results, which can also provide automated comparisons between different circuits and subcircuits. For instance, Figure 4a shows the histogram for the QFT circuit. We can see in the histograms that the uncut circuit (blue line) has a mean of 0.44 and a small standard deviation (e.g. a large peak than the others), which indicates a higher number of gray values in the heatmap than for the other circuits. Subcircuit 0 (black line) reduces the peak and shifts some values to a lower QVF, increasing the standard deviation and reducing the mean with respect to the uncut circuit. This result indicates a higher number of green values in the heatmap, as can be seen in Figure 3b. Subcircuit 1 (red line) has the same mean of the uncut circuit with a higher standard deviation, reducing the number of dubious outputs (i.e., gray squares in the heatmaps). Finally, subcircuit 2 (green line) shifts the mean to 0.5, indicating much more sensitivity to faults than the other ones.

Figure 4c and 4b show the histogram for DJ and BV respectively. We do not provide the heatmaps and a detailed evaluation for both circuits due to space restraints, however, all data is publicly available in our repository [28]. Both uncut circuits perform similarly, which is expected since BV is an extension of DJ [26]. Subcircuit 0 is also more critical for both circuits, shifting the mean slightly to the right while reducing the number of dubious outputs by increasing the standard deviation. Thus, increasing the number of harmless faults as well as the number of critical faults. Subcircuit 1, for BV, is the best performing subcircuit regarding the reliability, providing a mean of only 0.38. For DJ, subcircuit 1 provides a minor improvement with respect to the uncut one, shifting the mean from 0.49 to 0.42.

B. Selective Hardening

Although effective hardening solution to transient faults for quantum circuits are still unavailable, we can estimate the impact of a potential selective hardening. We consider that a hardened circuit will not allow faults to propagate and we assume the cost of a potential hardening technique to be linearly dependent on the number of gates and qubits in the circuit (similar to replication in traditional computing).

We show in Figure 5 the histograms for the three algorithms tested if one of the subcircuits is protected. We assume that a protected subcircuit will produce the same QVF as the fault-free execution (faults are masked), which corresponds to the heatmap where $(\theta = 0, \phi = 0)$. We choose not to use QVF=0 since we still assume an intrinsically noisy computation (NISQ era), which results in a QVF close to zero but not exactly zero. Thus, to visualize the impact of protecting one subcircuit, we replace the QVF for each fault in that specific subcircuit with the value of a fault-free execution, while retaining the QVF values for faults in the other unprotected subcircuits.

Figure 5a shows the result of protecting QFT subcircuit 0 in black lines, subcircuit 1 in red lines, and subcircuit 2 in green lines. Protecting subcircuits 1 and 2 provides a significant amount of protection, reducing the mean to about 0.3 with a small standard deviation. However, subcircuit 0 provides the best level of protection, with a mean of about 0.2. It is worth noting that subcircuit 2 is the most critical one as shown in Figure 4a, but subcircuit 0 is the larger one while subcircuit 2 is the smaller one (as detailed in Section IV-A). Then, one should take into account not only the criticality but also the size of each subcircuit when choosing which one to protect.

Moreover, if the overhead of a protection technique is based on the circuit width (i.e., a greater number of qubits is needed to execute the same circuit), protecting subcircuit 0 should have the same overhead as protecting subcircuit 2 since both have 3 qubits. If the protecting overhead is based on the number of gates (which means it increases the depth of the circuit, requiring higher quality hardware, especially in terms of coherence times), then subcircuit 0 overhead is only about 0.55 times the overhead of protecting the uncut circuit, but 3.7 times the overhead of protecting subcircuit 2.

For BV and DJ, Figures 5b and 5c present the QVF assuming protection of subcircuit 0 in black lines and of subcircuit 1 in red ones. For BV (Figure 5b), among all the injected faults on both subcircuits, those that can be classified as harmful (QVF > 0.55) amount to 40%. Of these, the highest concentration, corresponding to 82.2% of the harmful faults, is located in subcircuit 0. Thus, making subcircuit 0 4.6 times more likely to corrupt the final output than subcircuit 1. Performing the same calculation for DJ, whose QVF distribution is shown in Figure 5c, the amount of harmful faults is 40.6% of the total. The highest concentration of these is again in subcircuit 0, which accounts for 80% of the harmful faults. Hence, subcircuit 0 is 4.0 times more likely to corrupt the final output than subcircuit 1. If the protection technique is based solely on circuit depth, protecting subcircuits 0 may be slightly more efficient than protecting the uncut circuits. If the overhead of the protection technique is determined by the number of gates, the overhead of protecting subcircuit 0 with respect to the uncut circuit is 0.79 for BV and 0.77 for DJ.

Our results demonstrate the relevance of the cutting technique for quantum circuit reliability analysis and improvements. The significant difference in the QVF values between the circuit portions highlights that fault propagation is strongly dependent on the circuit portion. Our evaluation becomes, then, a viable criterion for selecting where to focus the hardening efforts to improve the protection efficiency.

VI. Conclusions

In this paper, we have seen that the circuit cutting technique, besides allowing for a large circuit to be executed into small quantum computers, can also be fruitfully exploited to improve reliability. We demonstrate that each subcircuit has indeed different fault propagation characteristics and fault sensitivities. Carefully selecting subcircuits to harden can potentially significantly mitigate the impact of faults by a fraction of the cost to harden the uncut circuit. Moreover, since the current cutting strategy neglects the reliability impact, one can devise new cutting strategies to improve the selective hardening impact on reliability and overhead.

REFERENCES

[1] L. K. Grover, "A fast quantum mechanical algorithm for database search," *arXiv e-prints*, pp. quant–ph/9 605 043, May 1996.

[2] S. Lloyd, M. Mohseni, and P. Rebentrost, "Quantum algorithms for supervised and unsupervised machine learning," 2013.

[3] A. Peruzzo, J. McClean, P. Shadbolt, M.-H. Yung, X.-Q. Zhou, P. J. Love, A. Aspuru-Guzik, and J. L. O'Brien, "A variational eigenvalue solver on a photonic quantum processor," *Nature Communications*, vol. 5, no. 1, p. 4213, 2014. [Online]. Available: https://doi.org/10.1038/ncomms5213

[4] R. Mullin, "Let's talk about quantum computing in drug discovery," *C&EN Global Enterprise*, vol. 98, no. 35, pp. 20–22, 09 2020. [Online]. Available: https://doi.org/10.1021/cen-09835-feature2

[5] e. a. MD SAJID ANIS, "Qiskit: An open-source framework for quantum computing," 2021.

[6] A. Li, O. Subasi, X. Yang, and S. Krishnamoorthy, *Density Matrix Quantum Circuit Simulation via the BSP Machine on Modern GPU Clusters*. IEEE Press, 2020.

[7] S. Bravyi, M. Englbrecht, R. König, and N. Peard, "Correcting coherent errors with surface codes," *npj Quantum Information*, vol. 4, no. 1, p. 55, Oct 2018. [Online]. Available: https://doi.org/10.1038/s41534-018-0106-y

[8] C. Chamberland, A. Kubica, T. J. Yoder, and G. Zhu, "Triangular color codes on trivalent graphs with flag qubits," *New Journal of Physics*, vol. 22, no. 2, p. 023019, Feb 2020. [Online]. Available: http://dx.doi.org/10.1088/1367-2630/ab68fd

[9] A. D. Corcoles, J. M. Chow, J. M. Gambetta, C. Rigetti, J. R. Rozen, G. A. Keefe, M. Beth Rothwell, M. B. Ketchen, and M. Steffen, "Protecting superconducting qubits from radiation," *Applied Physics Letters*, vol. 99, no. 18, p. 181906, 2011. [Online]. Available: https://doi.org/10.1063/1.3658630

[10] L. Cardani, F. Valenti, N. Casali, G. Catelani, T. Charpentier, M. Clemenza, I. Colantoni, A. Cruciani, G. D'Imperio, L. Gironi, L. Grünhaupt, D. Gusenkova, F. Henriques, M. Lagoin, M. Martinez, G. Pettinari, C. Rusconi, O. Sander, C. Tomei, A. V. Ustinov, M. Weber, W. Wernsdorfer, M. Vignati, S. Pirro, and I. M. Pop, "Reducing the impact of radioactivity on quantum circuits in a deep-underground facility," *Nature Communications*, vol. 12, no. 1, p. 2733, 2021. [Online]. Available: https://doi.org/10.1038/s41467-021-23032-z

[11] J. M. Martinis, "Saving superconducting quantum processors from decay and correlated errors generated by gamma and cosmic rays," *npj Quantum Information*, vol. 7, no. 1, p. 90, 2021. [Online]. Available: https://doi.org/10.1038/s41534-021-00431-0

[12] Z. Chen, K. J. Satzinger, J. Atalaya, A. N. Korotkov, A. Dunsworth, D. Sank, C. Quintana, M. McEwen, R. Barends, P. V. Klimov, S. Hong, C. Jones, A. Petukhov, D. Kafri, S. Demura, B. Burkett, C. Gidney, A. G. Fowler, A. Paler, H. Putterman, I. Aleiner, F. Arute, K. Arya, R. Babbush, J. C. Bardin, A. Bengtsson, A. Bourassa, M. Broughton, B. B. Buckley, D. A. Buell, N. Bushnell, B. Chiaro, R. Collins, W. Courtney, A. R. Derk, D. Eppens, C. Erickson, E. Farhi, B. Foxen, M. Giustina, A. Greene, J. A. Gross, M. P. Harrigan, S. D. Harrington, J. Hilton, A. Ho, T. Huang, W. J. Huggins, L. B. Ioffe, S. V. Isakov, E. Jeffrey, Z. Jiang, K. Kechedzhi, S. Kim, A. Kitaev, F. Kostritsa, D. Landhuis, P. Laptev, E. Lucero, O. Martin, J. R. McClean, T. McCourt, X. Mi, K. C. Miao, M. Mohseni, S. Montazeri, W. Mruczkiewicz, J. Mutus, O. Naaman, M. Neeley, C. Neill, M. Newman, M. Y. Niu, T. E. O'Brien, A. Opremcak, E. Ostby, B. Pató, N. Redd, P. Roushan, N. C. Rubin, V. Shvarts, D. Strain, M. Szalay, M. D. Trevithick, B. Villalonga, T. White, Z. J. Yao, P. Yeh, J. Yoo, A. Zalcman, H. Neven, S. Boixo, V. Smelyanskiy, Y. Chen, A. Megrant, J. Kelly, and G. Q. AI, "Exponential suppression of bit or phase errors with cyclic error correction," *Nature*, vol. 595, no. 7867, pp. 383–387, 2021. [Online]. Available: https://doi.org/10.1038/s41586-021-03588-y

[13] L. Grünhaupt, N. Maleeva, S. T. Skacel, M. Calvo, F. Levy-Bertrand, A. V. Ustinov, H. Rotzinger, A. Monfardini, G. Catelani, and I. M. Pop, "Loss mechanisms and quasiparticle dynamics in superconducting microwave resonators made of thin-film granular aluminum," *Phys. Rev. Lett.*, vol. 121, p. 117001, Sep 2018. [Online]. Available: https://link.aps.org/doi/10.1103/PhysRevLett.121.117001

[14] A. P. Vepsäläinen, A. H. Karamlou, J. L. Orrell, A. S. Dogra, B. Loer, F. Vasconcelos, D. K. Kim, A. J. Melville, B. M. Niedzielski, J. L. Yoder, S. Gustavsson, J. A. Formaggio, B. A. VanDevender, and W. D. Oliver, "Impact of ionizing radiation on superconducting qubit coherence," *Nature*, vol. 584, no. 7822, pp. 551–556, 2020. [Online]. Available: https://doi.org/10.1038/s41586-020-2619-8

[15] C. D. Wilen, S. Abdullah, N. A. Kurinsky, C. Stanford, L. Cardani, G. D'Imperio, C. Tomei, L. Faoro, L. B. Ioffe, C. H. Liu, A. Opremcak, B. G. Christensen, J. L. DuBois, and R. McDermott, "Correlated charge noise and relaxation errors in superconducting qubits," *Nature*, vol. 594, no. 7863, pp. 369–373, 2021. [Online]. Available: https://doi.org/10.1038/s41586-021-03557-5

[16] W. Tang, T. Tomesh, M. Suchara, J. Larson, and M. Martonosi, "CutQC: using small quantum computers for large quantum circuit evaluations," in *Proceedings of the 26th ACM International Conference on Architectural Support for Programming Languages and Operating Systems*. ACM, apr 2021. [Online]. Available: https://doi.org/10.1145%2F3445814.3446758

[17] T. Peng, A. W. Harrow, M. Ozols, and X. Wu, "Simulating large quantum circuits on a small quantum computer," *Physical Review Letters*, vol. 125, no. 15, oct 2020. [Online]. Available: https://doi.org/10.1103%2Fphysrevlett.125.150504

[18] M. H. Devoret and R. J. Schoelkopf, "Superconducting circuits for quantum information: An outlook," *Science*, vol. 339, no. 6124, pp. 1169–1174, 2013. [Online]. Available: https://www.science.org/doi/abs/10.1126/science.1231930

[19] L. Hu, Y. Ma, W. Cai, X. Mu, Y. Xu, W. Wang, Y. Wu, H. Wang, Y. P. Song, C.-L. Zou, S. M. Girvin, L.-M. Duan, and L. Sun, "Quantum error correction and universal gate set operation on a binomial bosonic logical qubit," *Nature Physics*, vol. 15, no. 5, pp. 503–508, Feb. 2019. [Online]. Available: https://doi.org/10.1038/s41567-018-0414-3

[20] R. Barends, J. Wenner, M. Lenander, Y. Chen, R. C. Bialczak, J. Kelly, E. Lucero, P. O. Malley, M. Mariantoni, D. Sank, H. Wang, T. C. White, Y. Yin, J. Zhao, A. N. Cleland, J. M. Martinis, and J. J. A. Baselmans, "Minimizing quasiparticle generation from stray infrared light in superconducting quantum circuits," *Applied Physics Letters*, vol. 99, no. 11, p. 113507, 2011. [Online]. Available: https://doi.org/10.1063/1.3638063

[21] M. McEwen, L. Faoro, K. Arya, A. Dunsworth, T. Huang, S. Kim, B. Burkett, A. Fowler, F. Arute, J. C. Bardin, A. Bengtsson, A. Bilmes, B. B. Buckley, N. Bushnell, Z. Chen, R. Collins, S. Demura, A. R. Derk, C. Erickson, M. Giustina, S. D. Harrington, S. Hong, E. Jeffrey, J. Kelly, P. V. Klimov, F. Kostritsa, P. Laptev, A. Locharla, X. Mi, K. C. Miao, S. Montazeri, J. Mutus, O. Naaman, M. Neeley, C. Neill, A. Opremcak, C. Quintana, N. Redd, P. Roushan, D. Sank, K. J. Satzinger, V. Shvarts, T. White, Z. J. Yao, P. Yeh, J. Yoo, Y. Chen, V. Smelyanskiy, J. M. Martinis, H. Neven, A. Megrant, L. Ioffe, and R. Barends, "Resolving catastrophic error bursts from cosmic rays in large arrays of superconducting qubits," *Nature Physics*, vol. 18, no. 1, pp. 107–111, Jan. 2022. [Online]. Available: https://doi.org/10.1038/s41567-021-01432-8

[22] D. Oliveira, E. Giusto, E. Dri, N. Casciola, B. Baheri, Q. Guan, B. Montrucchio, and P. Rech, "Qufi: a quantum fault injector to measure the reliability of qubits and quantum circuits," *arXiv preprint arXiv:2203.07183*, 2022.

[23] M. A. Perlin, Z. H. Saleem, M. Suchara, and J. C. Osborn, "Quantum circuit cutting with maximum-likelihood tomography," *npj Quantum Information*, vol. 7, no. 1, pp. 1–8, 2021.

[24] D. Deutsch and R. Jozsa, "Rapid solution of problems by quantum computation," *Proceedings of the Royal Society of London. Series A: Mathematical and Physical Sciences*, vol. 439, no. 1907, pp. 553–558, Dec. 1992. [Online]. Available: https://doi.org/10.1098/rspa.1992.0167

[25] R. Cleve, A. Ekert, C. Macchiavello, and M. Mosca, "Quantum algorithms revisited," *Proceedings of the Royal Society of London. Series A: Mathematical, Physical and Engineering Sciences*, vol. 454, no. 1969, pp. 339–354, Jan. 1998. [Online]. Available: https://doi.org/10.1098/rspa.1998.0164

[26] E. Bernstein and U. Vazirani, "Quantum complexity theory," *SIAM Journal on Computing*, vol. 26, no. 5, pp. 1411–1473, 1997. [Online]. Available: https://doi.org/10.1137/S0097539796300921

[27] D. Coppersmith, "An approximate fourier transform useful in quantum factoring," 2002. [Online]. Available: https://arxiv.org/abs/quant-ph/0201067

[28] "Repository with this paper's data," https://github.com/QuTAM/IOLTS2022_QC_Cutting_Data, May 2022.